CrystEngComm

ROYAL SOCIETY OF CHEMISTRY

COMMUNICATION

View Article Online
View Journal | View Issue

Cite this: *CrystEngComm*, 2021, **23**, 1550

Received 11th December 2020,
Accepted 30th January 2021

DOI: 10.1039/d0ce01799j

rsc.li/crystengcomm

A selective cocrystallization separation method based on non-covalent interactions and its application†

Na Wang,[a] Jingkang Wang,[ab] Xin Huang,*[ab] Ting Wang,[ab] Xin Li,[a] Jinyue Yang,[a] Ying Bao,[ab] Qiuxiang Yin[ab] and Hongxun Hao*[abc]

The purification of isomer monomers with high purity is extremely important, particularly in the fine chemical industry, pharmaceutical industry, and so on. Herein, a selective cocrystallization (SCoC) technology based on non-covalent interactions between the target compound and cocrystal conformers was developed to effectively separate isomer mixtures. The unique and efficient selectivity nature of conformers and the general applicability of the selective cocrystallization method was tested through separating and purifying cresol isomer mixtures, pyridinecarboxamide isomer mixtures, and *cis*–/*trans*-butenedioic acid mixtures. Moreover, the nature of selective recognition to cocrystallize was confirmed both in the solution and solid states. Thus, this study demonstrates the feasibility of this novel SCoC technology, which is a new method for separating isomer mixtures.

The effective separation of isomer mixtures into pure species is a critical and challenging industrial process and has always been highly concerned by scientists and researchers. An effective separation approach leading to highly pure isomer monomers is of utmost importance,[1,2] in particular, for the fine chemical industry, pharmaceutical industry, materials, *etc.* However, since the molecular characteristics (including molecular volume, molecular shape, dipole moment, and polarization strength) of isomer monomer molecules are very close, the isomers have little difference in physical properties[3] (*e.g.*, boiling point, density, and solubility), which makes the separation of isomers difficult by conventional methods.[3]

At present, alternative separation technologies developed for the isomer mixtures include the adsorptive separation method using selective ordered porous solid adsorbents, such as zeolitic imidazolate frameworks (ZIFs),[4] metal–organic frameworks (MOFs) materials[5,6] (also known as porous coordination polymers), covalent organic frameworks (COFs),[7,8] hydrogen-bonded organic frameworks (HOFs),[9,10] hybrid mixed-matrix membranes,[11] and MOF-based membranes;[1,12,13] the separation method using nonporous organic solid materials;[14,15] the separation method using nonporous adaptive crystals;[16–18] special distillation (*e.g.*, molecular distillation,[19] and extractive distillation[20]); the chromatographic separation (*e.g.*, supercritical fluid chromatography separation[21,22]); capillary electrophoresis (*e.g.*, capillary zone electrophoresis[23,24] and capillary electrochromatography[25–27]); chemical (kinetic) resolution;[28,29] and (non-selective) cocrystallization technology.[30] However, the above-mentioned separation and/or purification methods have certain disadvantages in industrial applications, such as difficult to scale-up, high energy consumption, and high equipment and installation costs. Therefore, it is of great significance to explore new energy-friendly and easy-to-scale-up strategies for the purification of isomer mixtures. As an emerging method of using non-covalent interactions between the target compound and conformers (CCFs), the cocrystallization method has the potential to separate isomer mixtures into pure monomers with high purity. Although this method has been reported to separate[31–33] compounds that cannot form salts while having high purity requirements (such as high purity active pharmaceutical ingredients), the mutual recognition and its selectivity for the formation of cocrystals between the target compounds and different conformers, which is different from the single target molecule and causes change in the lattice energy and/or dissolution properties of the target molecule, were not revealed and well understood. The general rules for the selection of conformers that can be used to form cocrystals with each target monomer were not

[a] *National Engineering Research Center of Industrial Crystallization Technology, School of Chemical Engineering and Technology, Tianjin University, Tianjin, 300072, P. R. China. E-mail: x_huang@tju.edu.cn, hongxunhao@tju.edu.cn*
[b] *Collaborative Innovation Center of Chemical Science and Engineering, Tianjin, 300072, P. R. China*
[c] *School of Chemical Engineering and Technology, Hainan University, Haikou, 570228, P. R. China*

† Electronic supplementary information (ESI) available. CCDC 2024768 and 2024770. For ESI and crystallographic data in CIF or other electronic format see DOI: 10.1039/d0ce01799j

established.[34,35] Therefore, the development of the cocrystallization method is still mainly dependent on trial-and-error experiments, which are quite time-consuming.[35]

Herein, we introduced a method based on the principles of supramolecular chemistry and crystal engineering for the resolution of isomer mixtures *via* the selective cocrystallization technology (Scheme 1). The selective cocrystals refer to those cocrystals that coformers can only selectively interact with a certain isomer monomer *via* non-covalent interactions and that have higher and specific selectivity than these common and non-selective cocrystals. Moreover, the crystallization process that forms selective cocrystals is called "selective cocrystallization (SCoC)". Moreover, we also found that the selectivity can not only be observed in the solid-state cocrystals but also in the supramolecular synthons that will be used as precursors of these selective cocrystals in the solution state. Cocrystallization typically depends on non-covalent interactions between different molecules,[36] such as H-bonding, halogen bonding,[37–39] π-stacking, and charge-transfer,[40–42] which are universal. The selective cocrystallization (SCoC) technology developed in this study can be industrially used for the separation of different types of isomer mixtures.

The target compounds, cresol isomers (*i.e.*, *m*-cresol, MC; *o*-cresol, OC and *p*-cresol, PC, respectively. See in Fig. S1†), used as a model system to develop the SCoC technology are important chemicals and are in huge demand for the manufacturing of antioxidants, phenolic resins, plasticizers, inhibitors, agricultural chemicals, antiseptics, disinfectants, and surfactants but difficult to separate.[43–45] They all have strong H-bonding donor and/or acceptor sites. Moreover, urea (U), oxalic acid (OXA), and piperazine (PP) (see in Fig. S1†) were selected as CCFs for SCoC. Moreover, SCoC in the solution and solid states was studied, and the technology was applied to the separation of isomer mixtures. The selective cocrystallization has a low dependency on the solvents as it can be carried out in toluene or other low-polar organic solvents or even without solvents.

Cocrystallization experiment (Scheme 1) results showed that U has significant selectivity towards MC and OC, while OXA has opposite but prominent selectivity towards PC. When the selective CCF I (U) was added to the cresol mixture (only containing MC and PC since OC can be removed by distillation in advance or only containing OC and PC), only MC (or OC) combined with U to form cocrystals and precipitated out, while PC does not interact with U and remained in the mother liquor, as shown in the process (1) of Scheme 1. Similarly, when CCF II (OXA) was added to the same cresol mixture, only PC formed cocrystal with OXA and precipitated out, while MC remained in the mother liquor, as shown in the process (2) of Scheme 1. Interestingly, when CCF III (PP) was added to the cresol mixture, both MC and PC combined with PP to form cocrystals. However, the melting points of these two cocrystals were quite different (MC_PP cocrystal: 61.7 °C; PC_PP cocrystal: 92.6 °C, Fig. S2†). Moreover, no selectivity phenomena were observed from CCF III (PP), as shown in the process (3) of Scheme 1.

The MC_U cocrystal and OC_U cocrystal exhibited similar physiochemical properties (see Fig. 1 and Fig. S2–S7†) and crystal structures (Fig. 2, S8 and S10 and Tables S1 and S2†). Moreover, single-crystal X-ray analyses showed that PP also exhibited micro-level selectivity towards cresol monomers. In these selective cocrystallization systems, U, as an H-bonding acceptor, can selectively form cocrystals with MC and OC in a stoichiometric ratio of 1 : 1, while it cannot form cocrystals with PC. There are three different types of supramolecular synthons: two supramolecular heterosynthons formed by U and MC/OC (*i.e.*, Synthon I, O–H···O, and Synthon II, N–H···O, Fig. 2), and one supramolecular homosynthon, formed by two self-complementary functional groups (*i.e.*, urea homodimers, Synthon III, N–H···O), which form one type of diamond-shaped one-dimensional LSAMs (long-range synthon Aufbau modules, LSAMs (1D)),[46–49] as shown in Fig. 2a and b. The LSAMs (1D) were extended into two-dimensional LSAMs (LSAMs (2D), Fig. S9a and b†) by π-stacking and H-bonding in Synthon III. The OXA

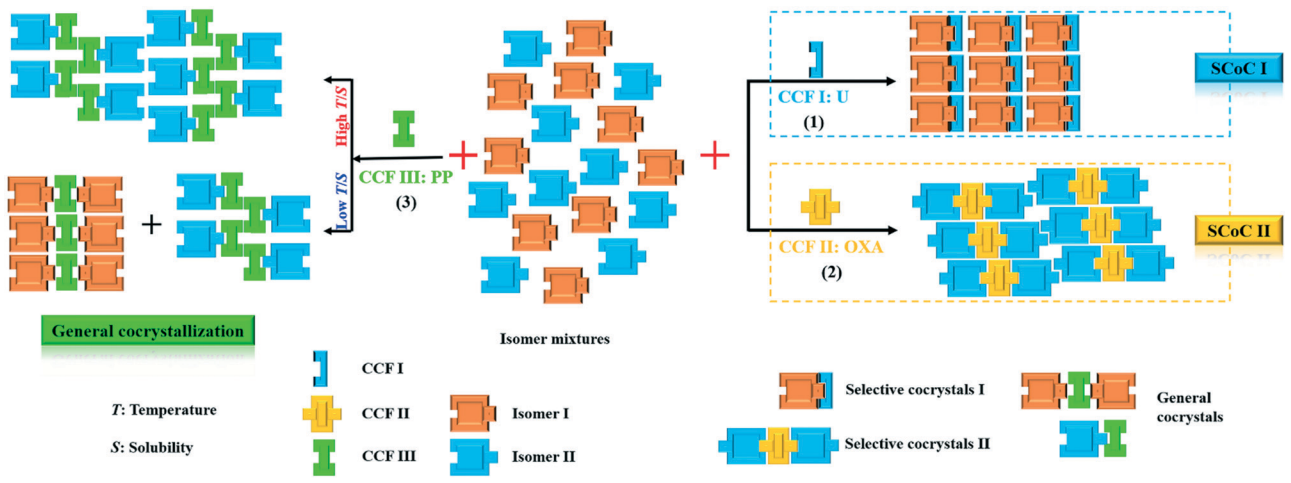

Scheme 1 Ways to apply the SCoC technology for the resolution of the mixtures of isomers.

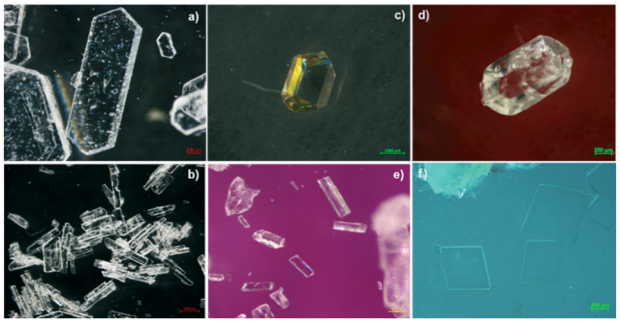

Fig. 1 Single crystals of a) MC_U cocrystal exhibiting a regular hexagonal shape, b) OC_U cocrystal exhibiting a regular rectangular, c) MC_PP cocrystal exhibiting a regular prism shape, d) OC_PP cocrystal exhibiting a regular prism shape, e) PC_PP cocrystal exhibiting long columnar and f) PC_OXA cocrystal exhibiting regular rhombus flakes.

conformer, as a strong H-bonding donor, can selectively form cocrystal (PC_OXA cocrystal) only with PC in a stoichiometric ratio of 1 : 2, while it cannot form cocrystals with MC and OC. Moreover, two types of supramolecular heterosynthons form LSAM (1D) (Fig. 2f) with a cyclic hydrogen bonding topology ($R_4^4(14)$) are stacked into LSAMs (2D) with a step-like architecture under π-stacking, as shown in Fig. S9f.† More interestingly, the PP molecule can act as both an H-bonding donor and acceptor. Although it can form cocrystals with all three cresol isomers in certain stoichiometric ratios, the formed cocrystals exhibited some selectivity: PP can form MC_PP and OC_PP cocrystals with MC and OC in the ratio of 1 : 2, while it can form PC_PP cocrystals with PC in the ratio of 1 : 1, which means that the PC molecule cannot form cocrystals with a PP molecule in a stoichiometric ratio of 1 : 2. Furthermore, the LSAMs (1D) (Fig. 2c and d) with a ladder-like architecture is the outstanding structural features of MC_PP and OC_PP cocrystals, which contains two supramolecular heterosynthons (Synthon I, O–H···N and Synthon II, N–H···π) by different but complementary functional groups. In addition, the LSAMs (1D) form LSAMs (2D) in an inverted V-shape, as shown in Fig. S9c and d.† On the contrary, the PC_PP cocrystal exhibited variability because it is composed of two supramolecular heterosynthons (Synthon I, O–H···N and Synthon II, N–H···π) and one supramolecular homosynthon (Synthon III, N–H···N), which first form LSAMs (1D) in a herringbone cross structure (Fig. 2e). Then, due to the π-stacking, two herringbone LSAMs (1D) chains in opposite directions form LSAMs (2D), as shown in Fig. S9e.†

To investigate the intermolecular interactions between the cresol molecules and their selective conformers in the solution, nuclear magnetic resonance (NMR) and attenuated total reflectance Fourier transformed infrared spectroscopy (ATR-FTIR) techniques were applied. The concentration-dependent ^{1}H NMR data showed that the intermolecular interactions of cocrystals became stronger and more clear with the amount of cocrystals (or host and CCFs with a certain stoichiometric ratio) added (as shown in Fig. 3, S11 and S12†). Under the circumstance of no cocrystal formation, the ^{1}H NMR data showed that the intermolecular interaction was weaker. Compared with the same CCFs that can form cocrystals, the change in the degree of the chemical shift of the related functional groups of cresols that cannot form cocrystals was either lower or not observable at the same concentration (as shown in Fig. S11 c–e†). In addition, comparing the concentration-dependent ^{1}H NMR data of MC (Fig. 3d and S12†) and selective cocrystals (Fig. 3a and b), it can be found that the change in the degree of the chemical shift of OH in selective cocrystals was much greater than that in MC under the same concentration. These results underline a strong association between MC/OC and U, and PC and OXA, respectively. Moreover, these data demonstrate that cresol molecules and the selective CCFs can selectively bind in the solution, which also confirms that these selective supramolecular synthons already exist as precursors in the

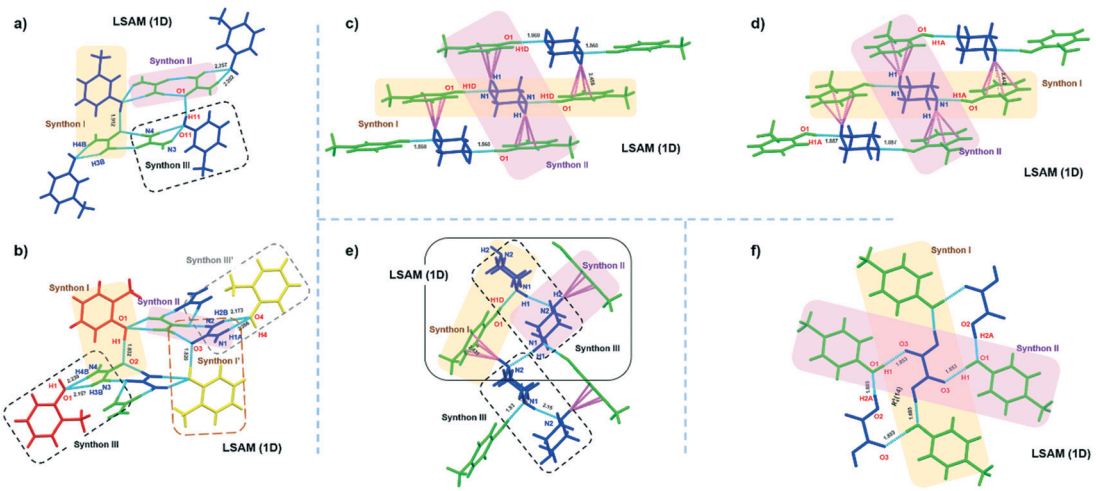

Fig. 2 1D LSAMs of cocrystals, a) MC_U, b) OC_U, c) MC_PP, d) OC_PP, e) PC_PP, and f) PC_OXA, respectively. The molecules are coloured by symmetry equivalence method, and the light blue dotted line (representing X–H···Y type) and light purple dotted line (representing π···H type) indicated different types of H-bonding in the cocrystals, respectively.

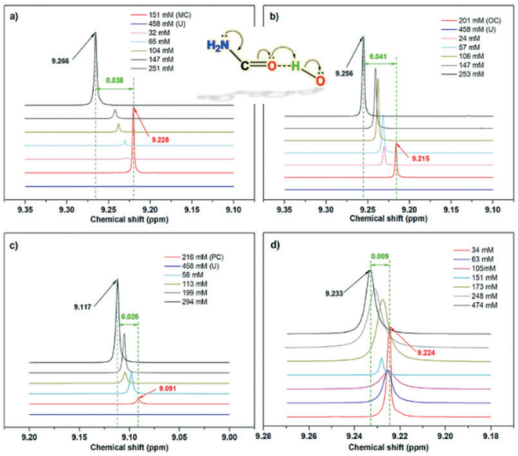

Fig. 3 The concentration-dependent ^{1}H NMR data of OH (cresols) in DMSO-d6. a) MCU cocrystals, b) OCU cocrystals, c) PC + U, and d) MC.

solution and carry over into the final selective cocrystals. The ATR-FTIR data of the solution containing cresol isomers and CCFs, with a certain ratio at numerous temperatures, showed that the content of the supramolecular synthons and the strength of intermolecular interactions in the solution are temperature-dependent.[50,51]

In the solution or solid-state, the specific selective recognition of cresol and its corresponding CCFs can be used for the effective separation of isomer mixtures, particularly for the effective separation of MC and PC. Specifically, U can only combine with MC, and hence can be used to selectively separate the mixture containing MC/PC with a certain molar ratio (*e.g.*, 1 : 0.5, 1 : 1, 1 : 2, and 1 : 5) since 1 : 1 cocrystal MC_U can be formed with high yield and purity. Further, OXA can selectively interact only with PC in the cresol mixture containing MC and PC since 2 : 1 cocrystal PC_OXA can be formed with high yield and purity. All the products were confirmed by PXRD and GC (Fig. S13–S15†). Notably, these selective cocrystals formed by the SCoC technology were up to 99.5% pure. With these experiments, we demonstrated that the SCoC technology could be applied to separate isomer mixtures into monomers with high purity *via* the formation of cocrystals.

The formation of selective cocrystals was also demonstrated in the solid-state by using neat grinding (NG) or liquid-assisted grinding (LAG) method. Particularly, competitive milling experiments were performed by mixing 1 equivalent of MC and/or PC with 1 equivalent of U and/or OXA, respectively. PXRD analyses (Fig. S16†) showed that only MC_U cocrystals and PC_OXA cocrystals could be formed, respectively.

To test the general applicability of the SCoC design based on H-bonding, some other CCFs, such as thiourea (TU), imidazole (IMZ), malonic acid (MAA), and succinic acid (SUA) that possess structures similar to that of conformers having selectivity (mentioned above), were applied to cocrystallize with MC and/or PC. PXRD analyses showed that thiourea and other dicarboxylic acids cannot form selective cocrystals, regardless of the cocrystallization methods used (*e.g.*, NG or LAG, solution crystallization, and melt crystallization) (Fig. S17†). However, imidazole (IMZ) can combine with MC, OC, and PC (Fig. S4†). Moreover, to verify the applicability of the idea developed in this study, the SCoC technology was also applied for the separation of N-heterocyclic isomers, *e.g.*, (2,3,4-) pyridinecarboxamide isomers, and unsaturated fatty acids, *e.g.*, *cis*–/*trans*-butenedioic acid or maleic/fumaric acid. PXRD analyses (Fig. S18†) showed that IMZ could only cocrystallize with 2-pyridinecarboxamide (2-PCAD) to form new substances, and it cannot cocrystallize with nicotinamide (3-PCAD) and isonicoinamide (4-PCAD), which exhibited selective cocrystallization. Similarly, thiourea (TU) can cocrystallize with maleic acid (ML) to form cocrystal, while it cannot form new substances with fumaric acid (FM), which also shows selective cocrystallization (Fig. S20†). Additionally, the PXRD patterns of monomers simulated by single-crystal crystallography were basically the same as the experimental PXRD patterns, and upon comparing it with the simulated PXRD patterns, the grinding products showed new characteristic diffraction peaks (Fig. S22 and S23†). Therefore, it can be deduced that the ability of selective recognition between the molecules is ubiquitous, and it is the foundation of selective cocrystallization.

Conclusions

In conclusion, we reported an innovative SCoC technology for the efficient separation of mixtures through different intrinsic selection natures of selective conformers towards different compounds. Here, this concept was applied for the separation of cresol isomers, and cresol monomers with high purity were obtained. Moreover, this inherent and unique selectivity was the essence of the selective cocrystallization technology, both in the solution and solid states. Overall, this unique selectivity makes the SCoC technology a general approach with high-efficiency separation capabilities, which possesses great potential for industrial applications in the field of isomer mixture separation.

Conflicts of interest

There are no conflicts to declare.

Acknowledgements

This work was supported by the National Natural Science Foundation of China [No.21978201].

Notes and references

1 X. Li, Y. Liu, J. Wang, J. Gascon, J. Li and B. Van der Bruggen, *Chem. Soc. Rev.*, 2017, **46**, 7124–7144.
2 D. L. Ginand and R. D. Noble, *Science*, 2011, **332**, 674.
3 S. H. Kim, J. H. Park, E. M. Go, W. Kim and S. K. Kwak, *J. Ind. Eng. Chem.*, 2020, **85**, 276–281.
4 J. H. Clark, *Acc. Chem. Res.*, 2002, **35**, 791–797.

5 W. Cui, T. Hu and X. Bu, *Adv. Mater.*, 2020, **32**, 1806445.
6 Z. R. Herm, B. M. Wiers, J. A. Mason, J. M. Van Baten, M. R. Hudson, P. Zajdel, C. M. Brown, N. Masciocchi, R. Krishna and J. R. Long, *Science*, 2013, **340**, 960–964.
7 A. P. Cote, A. I. Benin, N. W. Ockwig, M. Okeeffe, A. J. Matzger and O. M. Yaghi, *Science*, 2005, **310**, 1166–1170.
8 A. Nagai, Z. Guo, X. Feng, S. Jin, X. Chen, X. Ding and D. Jiang, *Nat. Commun.*, 2011, **2**, 536.
9 S. Nandi, D. Chakraborty and R. Vaidhyanathan, *Chem. Commun.*, 2016, **52**, 7249–7252.
10 A. Karmakar, R. Illathvalappil, B. Anothumakkool, A. Sen, P. Samanta, A. V. Desai, S. Kurungot and S. K. Ghosh, *Am. Ethnol.*, 2016, **55**, 10667–10671.
11 Y. Yampolskii, *Macromolecules*, 2012, **45**, 3298–3311.
12 W. Li, Y. Zhang, Q. Li and G. Zhang, *Chem. Eng. Sci.*, 2015, **135**, 232–257.
13 G. Liu, A. Cadiau, Y. Liu, K. Adil, V. Chernikova, I.-D. Carja, Y. Belmabkhout, M. Karunakaran, O. Shekhah, C. Zhang, A. K. Itta, S. Yi, M. Eddaoudi and W. J. Koros, *Angew. Chem., Int. Ed.*, 2018, **57**, 14811–14816.
14 V. Kumar, T. Pilati, G. Terraneo, G. Ciancaleoni, A. Macchioni, G. Resnati and P. Metrangolo, *Angew. Chem., Int. Ed.*, 2018, **57**, 1327–1331.
15 P. Metrangolo, Y. Carcenac, M. Lahtinen, T. Pilati, K. Rissanen, A. Vij and G. Resnati, *Science*, 2009, **323**, 1461–1464.
16 Y. Wang, K. Xu, B. Li, L. Cui, J. Li, X. Jia, H. Zhao, J. Fang and C. Li, *Angew. Chem., Int. Ed.*, 2019, **58**, 10281–10284.
17 K. Jie, Y. Zhou, E. Li, R. Zhao and F. Huang, *Angew. Chem., Int. Ed.*, 2018, **57**, 12845–12849.
18 J.-R. Wu and Y.-W. Yang, *Angew. Chem.*, 2020, **59**, 2–14.
19 X. Guo, S. Wang, Z. Guo, Q. Liu, Z. Luo and K. Cen, *Appl. Energy*, 2010, **87**, 2892–2898.
20 M. Seiler, C. Jork, A. Kavarnou, W. Arlt and R. Hirsch, *AIChE J.*, 2004, **50**, 2439–2454.
21 L. T. Taylor, *Anal. Chem.*, 2008, **80**, 4285–4294.
22 D. R. Gere, *Science*, 1983, **222**, 253–259.
23 J. W. Jorgenson and K. D. Lukacs, *Science*, 1983, **222**, 266+.
24 T. M. Mcnerney, S. K. Watson, J.-H. Sim and R. L. Bridenbaugh, *J. Chromatogr. A*, 1996, **744**, 223–229.
25 F. Lelièvre, C. Yan, R. N. Zare and P. Gareil, *J. Chromatogr. A*, 1996, **723**, 145–156.
26 V. Pino, *et al.*, *Anal. Sep. Sci.*, 2015, 653–675.
27 M. M. Dittmann and G. P. Rozing, *J. Chromatogr. A*, 1996, **744**, 63–74.
28 S.-Z. Li, J. Shi, K. Yang and J. Luo, *Tetrahedron*, 2012, **68**, 8557–8563.
29 S. Zhou, J. Wang, X. Chen, J. L. Aceña, V. A. Soloshonok and H. Liu, *Angew. Chem., Int. Ed.*, 2014, **53**, 7883–7886.
30 M. Guillot, J. de Meester, S. Huynen, L. Collard, K. Robeyns, O. Riant and T. Leyssens, *Angew. Chem.*, 2020, **59**, 11303–11306.
31 O. Sánchez-Guadarrama, F. Mendoza-Navarro, A. Cedillo-Cruz, H. Jung-Cook, J. I. Arenas-García, A. Delgado-Díaz, D. Herrera-Ruiz, H. Morales-Rojas and H. Höpfl, *Cryst. Growth Des.*, 2016, **16**, 307–314.
32 E. Corradi, S. V. Meille, M. T. Messina, P. Metrangolo and G. Resnati, *Angew. Chem., Int. Ed.*, 2000, **39**, 1782–1786.
33 G. Springuel and T. Leyssens, *Cryst. Growth Des.*, 2012, **12**, 3374–3378.
34 K. H. Hsi, K. Chadwick, A. Fried, M. Kenny and A. S. Myerson, *CrystEngComm*, 2012, **14**, 2386–2388.
35 J. Urbanus, C. P. M. Roelands, D. Verdoes, P. J. Jansens and J. H. ter Horst, *Cryst. Growth Des.*, 2010, **10**, 1171–1179.
36 S. Aitipamula, R. Banerjee, A. K. Bansal, K. Biradha, M. L. Cheney, A. R. Choudhury, G. R. Desiraju, A. G. Dikundwar, R. Dubey, N. Duggirala, P. P. Ghogale, S. Ghosh, P. K. Goswami, N. R. Goud, R. R. K. R. Jetti, P. Karpinski, P. Kaushik, D. Kumar, V. Kumar, B. Moulton, A. Mukherjee, G. Mukherjee, A. S. Myerson, V. Puri, A. Ramanan, T. Rajamannar, C. M. Reddy, N. Rodriguez-Hornedo, R. D. Rogers, T. N. G. Row, P. Sanphui, N. Shan, G. Shete, A. Singh, C. C. Sun, J. A. Swift, R. Thaimattam, T. S. Thakur, R. Kumar Thaper, S. P. Thomas, S. Tothadi, V. R. Vangala, N. Variankaval, P. Vishweshwar, D. R. Weyna and M. J. Zaworotko, *Cryst. Growth Des.*, 2012, **12**, 2147–2152.
37 G. Cavallo, P. Metrangolo, R. Milani, T. Pilati, A. Priimagi, G. Resnati and G. Terraneo, *Chem. Rev.*, 2016, **116**, 2478–2601.
38 K. Rissanen, *CrystEngComm*, 2008, **10**, 1107–1113.
39 B. Pinter, N. Nagels, W. A. Herrebout and F. De Proft, *Chem. – Eur. J.*, 2013, **19**, 519–530.
40 L. Sun, Y. Wang, F. Yang, X. Zhang and W. Hu, *Adv. Mater.*, 2019, **31**, 1902328.
41 J. Wang, S. Zhang, S. Xu, A. Li, B. Li, L. Ye, Y. Geng, Y. Tian and W. Xu, *Adv. Opt. Mater.*, 2020, **8**, 1901280.
42 Y. Sun, Y. Lei, H. Dong, Y. Zhen and W. Hu, *J. Am. Chem. Soc.*, 2018, **140**, 6186–6189.
43 K. Lee and C. Tan, *Ind. Eng. Chem. Res.*, 2000, **39**, 1035–1038.
44 L. Shiau, C. Huang and K. Liu, *Asia-Pac. J. Chem. Eng.*, 2012, **7**, S26–S31.
45 M. Lee and C. Chi, *J. Chem. Eng. Data*, 1993, **38**, 292–295.
46 A. Mukherjee, K. Dixit, S. P. Sarma and G. R. Desiraju, *IUCrJ*, 2014, **1**, 228–239.
47 M. Paul and G. R. Desiraju, *Angew. Chem., Int. Ed.*, 2019, **58**, 12027–12031.
48 R. Dubey, N. A. Mir and G. R. Desiraju, *IUCrJ*, 2016, **3**, 102–107.
49 C. O'dowd, J. D. Kennedy and M. Thornton-Pett, *J. Organomet. Chem.*, 2002, **657**, 20–39.
50 N. Wang, X. Huang, L. Chen, J. Yang, X. Li, J. Ma, Y. Bao, F. Li, Q. Yin and H. Hao, *IUCrJ*, 2019, **6**, 1064–1073.
51 N. Wang, H. Hao, H. Lu and R. Xu, *CrystEngComm*, 2017, **19**, 3746–3752.

